Metamorphism, Argon Depletion, Heat Flow and Stress on the Alpine Fault

CHRISTOPHER H. SCHOLZ

Department of Geological Sciences and Lamont-Doherty Geological Observatory of Columbia University, Palisades, New York 10964

JOHN BEAVAN

Lamont-Doherty Geological Observatory of Columbia University, Palisades, New York 10964

THOMAS C. HANKS

U. S. Geological Survey, 345 Middlefield Road, Menlo Park, California 94025

ABSTRACT

The Alpine fault of New Zealand is a major continental transform fault which has been uplifted on its southeast side 4 to 11 km within the last 5 m.y. This uplift has exposed the Haast schists, which have been metamorphosed from the adjacent Torlesse graywackes. The Haast schists increase in metamorphic grade from prehnite-pumpellyite facies 9-12 km from the fault through the chlorite and biotite zones of the greenschist facies to the garnet-oligoclase zone of amphibolite facies within 4 km of the fault. These metamorphic zone boundaries are subparallel to the fault for 350 km along the strike. The K-Ar and Rb-Sr ages of the schists increase with distance from the fault: from 4 m.y. within 3 km of the fault to approximately 110 m.y. 20 km from the fault. Field relations show that the source of heat that produced the argon depletion aureole was the fault itself, Adopting a friction model for the fault, and applying the known geological history of motion of the Alpine fault, we show that the metamorphism resulted from frictional heating during the 360 km right lateral slip on the Alpine fault during the Mesozoic (Rangitata) period of fault motion (140-120 m.y. ago). Fault motion began again in the Plio-Pleistocene Kaikoura orogeny, with 120 km of further right lateral slip and 4-11 km of uplift. Frictional heating during this episode produced the argon depletion. Quantitative models for both the metamorphism and argon depletion require that the frictional shear stress acting on the fault during both episodes of fault motion was at least 1-1.5 kbar.

INTRODUCTION

The state of stress within the lithosphere is fundamental to tectonics, yet it has remained enigmatic. Whereas the directions of the principal stresses at or near the earth's surface can be estimated with a variety of geological and geophysical techniques, the magnitude of deviatoric stresses that may exist within the lithosphere is as yet uncertain even to their order of magnitude. All that is firmly known at present is that shear stresses in tectonically active areas must exceed the stress drops of earthquakes, which are mainly confined to the range 10 to 100 bars [*Aki*, 1972; *Thatcher and Hanks*, 1973; *Kanamori and Anderson*, 1975; *Hanks*, 1977].

It is particularly important to know the value of the shear stress required to produce slip on crustal faults, since the frictional stresses at plate boundaries may well provide the primary forces for resisting the motion of the lithospheric plates. If these frictional stresses are low, of the order of earthquake stress drops, then their resulting resistance to plate motion is comparable to several likely driving forces [e.g., *Forsyth and Uyeda*, 1975]. If, on the other hand, they are of the order of kilobars, as suggested by laboratory measurements of rock friction [e.g., *Scholz*, 1977; *Byerlee*, 1978], then friction at plate boundaries becomes a major force resisting plate motion which may well require that basal shear stresses be an important driving force [*Hanks*, 1977; *Davies*, 1978].

If a fault has slipped a distance u, acting under an average shear stress $\bar{\tau}$, then the work per unit fault area, $\bar{\tau}u$, must be dissipated according to

$$\bar{\tau}u = E_s + \alpha A + Q$$

where E_s is the elastic energy radiated by earthquakes, αA is the energy required to produce new surfaces of area A and specific surface energy a, and Q is heat. Various arguments Can be advanced to indicate that the first *two* terms on the right hand side of this energy balance can be neglected with respect to the third, but we can at least say, conservatively, that

$$\bar{\tau} u < Q$$

If we can measure the frictional heat generated by fault slip, Q, and estimate the fault slip u, we can then obtain a lower bound on $\bar{\tau}$.

In this study we apply this approach to the Alpine fault of New Zealand, one of the major continental transcurrent faults. Within the last 5 m.y., 4 to 11 km of uplift on the southeast side of this fault has exposed a sequence of rocks (Haast schists) which have a metamorphic history that can be related ta two episodes of heating due to frictional sliding on the fault. We develop the evidence for this interpretation in more detail in the following section, but briefly, our reconstruction is as follows. Between 140 and 120 m.y. ago (Rangitata orogeny) some 360 km of right-lateral slip on the Alpine fault generated sufficient heat to metamorphose a thick sequence of eugeosynclinal graywackes adjacent to the fault. These metamorphic rocks (the Haast schists) were at that time deeply buried and formed part of a broad ductile shear zone. The highest metamorphic grade of the Haast schists, garnet-oligoclase zone of amphibolite facies, occurs adjacent to the fault, and the metamorphic grade decreases with distance from the fault, through the biotite and chlorite zones of the greenschist facies to prehnite-pumpellyite and pumpellyite-actinolite subschists that occur 9-12 km from the fault. The fault was reactivated about

5 m.y. ago (Kaikoura orogeny) during which a further 120 km of right-lateral slip occurred, accompanied by 4 to 11 km of uplift that exposed the Haast schists in what are now the Southern Alps. During the Kaikoura period of fault motion, frictional heating produced only a slight retrograde metamorphism in the Haast schists but was sufficient to almost completely degas these rocks of their radiogenic argon and deplete their micas of strontium and thereby reset their K-Ar and Rb–Sr ages to very young values near the fault.

In order to account for both the distribution of metamorphic isograds within the Haast schists and the distribution of their K–Ar ages, we have quantitatively modeled the frictional thermal events produced by both periods of fault motion. We find that within the permissible range of all variable parameters for both periods of fault motion, a minimum average value of 1 to 1.5 kb for the frictional stress on the Alpine fault.

GEOLOGICAL HISTORY OF THE HAAST SCHISTS

The South Island of New Zealand was a site of active subduction during the Mesozoic, as indicated by the arc terrane of the New Zealand geosyncline [*Landis and Bishop*, 1972]. The arc terrane is preserved in the southern part of the South Island (Figure 1). The Fiordland igneous complex in the west consists of a high T/P metamorphic terrane intruded by numerous calc-alkaline plutons, and is interpreted as the relic of the Mesozoic arc. To the east of this complex is a narrow zone of blueschists and ultramafics that abut a tectonic suture (Livingstone-Macpherson fault zone) that separates these rocks

from the voluminous eugeosynclinal sediments of the Torlesse group. The latter have been interpreted as trench sediments [*Landis and Bishop*, 1972].

At the culmination of this Rangitata orogeny the Otago schists, a broad NW-SE striking band of schists derived from the Torlesse group, were deformed and uplifted. The Otago schists outcrop in a broad NW-SE striking antiform. Their highest metamorphic grade, the biotite zone of the greenschist facies is found in the central part of their outcrop area, and their metamorphic grade decreases both to the NE and SW from this central zone. The Otago schists have K-Ar ages of 110-140 m.y. [*Harper* and *Landis*, 1967; *Sheppard et al.*, 19751 and they probably formed during a compressional event which produced shortening normal to the arc near the end of the Rangitata orogeny.

The arc terrane was subsequently offset 480 km by right-lateral slip on the Alpine fault [*Wellman*, 1955; *Suggate*, 19631. We thus see exposed in the northwest comer of the South Island a repetition of the entire arc sequence (Figure 1). There the Marlborough schists lie in the identical structural position as the Otago schists, and we interpret them as being their offset equivalents. We also notice that a swarm of lamprophyre dikes, dated at 120 m.y., has been offset 120 km by the Alpine fault [*Wellman and Cooper*, 19711. Therefore 360 km of fault motion must have occurred in the Mesozoic, between 140 to 120 m.y. B.P. Since the motion of the Alpine fault is presently oblique slip, with a component of thrust faulting superimposed on right-lateral strike-slip movement [*Clark and Wellman*, 1959; *Suggate*, 1963; *Scholz et al.*, 1973], the remaining 120 km of fault slip is assumed to have occurred in the last 5 m.y., that is, since the initiation of uplift of the

Southern Alps in the Kaikoura orogeny [*Suggate*, 19631. The present rate of motion on the fault is 5 cm/yr right lateral from sea floor spreading data [*Christoffel*, 1971; *Hayes* and *Talwani*, 19721 to 1 cm/yr from geological observations [*Clark and Wellman*, 19591. Vertical motions may be several mm/yr [*Suggate*, 1963, 1968].

The Haast (or Alpine) schists are petrographically similar to the Otago and Marlborough schists in that they are also metamorphic equivalents of the Torlesse group sediments. These pelitic schists, however, have a distinctly different tectonic and metamorphic history. The Haast schists outcrop between the Alpine fault and the main divide of the Southern Alps. In the southern part of their outcrop area, where they merge with the Otago schists. the folds tighten up and the fold axes are rotated (dextrally) into near parallelism with the Alpine fault as they approach the fault [*Grindley*, 19631. The intensity of deformation of these rocks increases towards the fault, and within a few km of the fault have a schistocity and lineation subparallel to the fault. The style of deformation of the Haast schists is in accord with their having been formed under conditions close to pure shear in the same sense as that which produced the motion on the Alpine fault, and we interpret them as the exposure, at an intermediate structural level, of a ductile shear zone associated with the early (Rangitata) period of motion on the Alpine fault. Furthermore, unlike the Otago and Marlborough schists, the Haast schists were not uplifted until the Kaikoura orogeny. morphic grade of the Haast schists also increases towards the Alpine fault. The metamorphic zone boundaries are subparallel. to the fault and their distance from the fault varies with the amount of uplift, which is generally greatest towards the south, judging from the present elevation of the Alps. In the

central Alps, from Arthur's Pass to Haast Pass, this relationship is the most regular (Figure 2). There garnet-oligoclase zone schists of the lowest amphibolite facies occur within a few km of the fault. The schists decrease in grade through the biotite and chlorite zones of the greenschist facies to prehnite-pumpellyite facies subschists which occur 9–12 km from the fault. Very close to the fault, isolated pegmatite dikes occur as concordant lenses in the garnet schists and are interpreted as being due to partial melting [Figure 2; *Grindley*, 1963]. The K-Ar and Rb–Sr ages of the Haast schists also show a regular relationship with the fault. In Figure 3, South Island K–Ar ages from *Sheppard et al.* [1975] are plotted as a function of distance from the Alpine fault. The oldest ages for the South Island are in the range 140–150 m.y., which probably dates the onset of Rangitata metamorphism; a second group of ages is in the range 100–120 m.y. which probably represents late Rangitata uplift and cooling [*Sheppard et al.*, 1975]. In contrast with the regional ages are a group of very young ages from the Haast schists just east of the Alpine fault. The K-Ar whole rock and biotite ages from the Haast schists between Arthur's Pass and Haast Pass are shown in Figure 4. These data indicate a strong argon depletion within 10–15 km of the fault, with a form very similar to that observed in contact metamorphic aureoles adjacent to intrusive magmatic bodies [*Rart*, 1964], except that the lateral extent of the depletion is much greater.

These distinctive patterns of metamorphism and argon depletion adjacent to the Alpine fault have long been recognized [*Mason*, 1961, 1962; *Hurley et al., 1962*; *Grindley*, 1963; *Aronson*, 1965; *Harper and Landis*, 1967; *Sheppard et al.*, 1975]. They were originally interpreted by *Mason* [1961, 1962], with

later elaboration due to *Harper and Landis* [1967], as the result of major (20 to 30 km) uplift and rotation/differential uplift of rocks whose metamorphic grade was originally established by their great depth of burial in the crust. Since the highest grade (highest temperature) metamorphism is closest to the fault, the K-Ar ages can be interpreted as the age at which the local temperature dropped beneath the Ar retention temperature during uplift, being the most recent for the highest temperature facies which require the largest temperature drop and were at the greatest original depth.

Sheppard et al. [1975], principally on the basis of the K-Ar ages and concentration of ^{40}Ar, argued that the single stage uplift model described above did not entirely explain the observations or otherwise meet separate constraints. They proposed a two-stage model in which the metamorphic grade of the Haast schists was established between 140 and 120 m.y. ago but the argon depletion resulted from rejuvenation of the Alpine fault 4 ± 2 m.y. ago. They concluded that the source of the heat necessary to establish the observed Ar retention pattern was the fault itself. In support of this two-stage model are the following points.

1. The lamprophyre dikes cut the schists with chilled contacts [*Grindley*, 1963], therefore metamorphism of the Haast schists occurred prior to 120 m.y., whereas the argon depletion occurred after 120 m.y. A two-stage process is thus required.

2. To explain the observed argon depletion spectrum by simple uplift, the uplift must have occurred progressively over the past 110 m.y., but no schist detritus is found in sediments to the west of the Alpine fault of

greater than Pliocene age [*Grindley*, 1963; *Suggate*, 1963]. The evidence is thus that most of the uplift of the Southern Alps occurred in the last 5 m.y.

3. The single stage uplift model requires that the K-Ar age be directly related to depth of burial and hence metamorphic grade of the schists. *Sheppard et al.* [1975], however, showed that K-Ar age is solely a function of distance from the fault and not of metamorphic grade. This is consistent with points 1 and 2 that metamorphism occurred in the Mesozoic and argon depletion in the Cenozoic.

4. In a simple uplift model the temperatures are insufficient to degas the argon in the way observed. Thus *Hurley et al.* [1962] calculated the argon diffusion parameters for biotite by using the uplift model and obtained results some ten orders of magnitude higher than that subsequently measured directly in the laboratory [*Fechtig and Kalbitzer*, 1966]. Any geothermal gradient sufficient to cause argon degassing in the upper part of the section would produce rocks of higher metamorphic grade in the lower part of the section than those that are actually found [*Sheppard et al.*, 1975].

5. If the metamorphic facies boundaries were originally horizontal, reflecting depth of burial, their present outcrop pattern, which indicates steeply dipping facies boundaries, requires a large rotation or differential uplift distributed through the schists. But no such rotation on either side of the fault is indicated for the lamprophyre dikes, which postdate the schists [*Grindley*, 1963; *Wellman and Cooper*, 1972] and the evidence is negative for distributed uplift on shear planes within the schists, since late and post-metamorphic folds have not been offset [*Grindley*, 1963].

A FRICTIONAL HEATING MODEL FOR MESOZOIC METAMORPHISM AND LATE CENOZOIC ARGON DEPLETION OF THE HAAST SCHISTS

Following the argument of *Sheppard et al.* [1975] that the argon depletion of the Haast schists must have involved frictional heating on the Alpine fault during its Plio-Pleistocene (Kaikoura) period of movement, we also note that the present metamorphic zone boundaries strongly suggest that the fault was a source of heat during the earlier (Rangitata) period of fault motion, and that the metamorphism resulted from frictional heating. Otherwise, according to our point 5 above, the present outcrop pattern of these metamorphic rocks is very difficult to explain.

In Figure 5 we schematically show the history of events in a series of vertical sections normal to the Alpine fault. Prior to 140 m.y. ago, we show the ancestral position of the Alpine fault in a region of normal geothermal gradient (Figure 5a). Between 140 and 120 m.y. (Figure 5b), the fault slipped 360 km and frictional heating elevated the isotherms in the vicinity of the fault, metamorphosing the adjacent rocks. We take 300°C as the prehnite/pumpellyite-greenschists facies boundary, and 450°C as the greenschist-amphibolite facies boundary, noting that below several km depth, where the metamorphism took place, these transition temperatures are almost independent of pressure [*Ernst*, 1975].

Our models will be constrained so that the 450° isotherm and 300° isotherm occur at distances L_1 and L_2 from the fault at a depth H, where L_1 and L_2 are the average distances from the fault of the amphibolite-greenschist and greenschist-prehnite/pumpellyite boundaries and H is the Cenozoic uplift of the Southern Alps.

From 120 to 5 m.y. there was no fault motion, the region cooled to a normal geothermal gradient, and the metamorphic facies boundairies were as shown in Figure 5c. The Kaikoura movements began 5 m.y. ago. with 120 km right-lateral slip and H km of uplift (Figure 5d). We will calculate the frictional heating produced by this slip, and using appropriate values of the diffusion parameters for argon from biotite, we will require that this predict the observed argon depletion profile. This second heisting event produced some retrograde metamorphism in the schists but did not alter the position of the zone boundaries [*Grindley*, 1963; *Sheppard et al.*, 1975]. Since the metamorphism is independent of the argon depletion, we will further constrain these models so that H and $\bar{\tau}$ are consistent in modelling both processes.

In the region of the central Southern Alps (Figure 2) the parameters L_1 = 4–5 km, L_2 = 9–12 km, and H = 4–11 km. The lower limit on H is given by the present elevation of the Southern Alps. the upper limit is derived from our calculations as the greatest depth at which biotite would retain radiogenic argon in the interval between the Rangitata and Kaikoura orogenies.

In the calculations that follow, we allow the parameters H, q_o, the ambient heat flow, and v, the velocity of fault slip, to vary within the allowable limits and calculate the lowest value of shear stress $\bar{\tau}$ required to produce the metamorphism and argon depletion. Two models of shear stress distribution were tried. In model A (Figure 6a) it was simply assumed that a shear stress $\bar{\tau}$ is applied to the fault from a depth 0.5 to 15.5 km. In the second model, B, it was assumed that the shear stress is governed by a

coefficient of friction μ so that $\tau = \mu\bar{\sigma}_n$ where $\bar{\sigma}_n$ is the effective normal stress on the fault. In this model then (Figure 6b), τ lncreases linearly with depth from 0.5 km to 15.5 km with a mean value, $\bar{\tau}$, at 8 km. Since heating from below 15 km did not significantly influence the results we assumed that $\bar{\tau} = 0$ at depths greater than 15.5 km.

In our models the source of heat was assumed to be a sheet or negligible thickness at the fault. Although, as described earlier. the Haa have undergone polyphase deformation that increases in intensity fault is approached, indicating that some of the transcurrent mo place by penetrative shear, early metamorphic (F_2) and post-metamorpnic (F_3) mesoscopic and macroscopic folds are not sheared out except within the mylonite zone [*Grindley,* 19631. We therefore conclude that the principal shearing was accommodated within the narrow (< 1 km thick) zone of mylonites at the fault *[Reed,* 19641. This agrees with the results of *Yuen et al.* [1978] who showed that the region of intense shear in a viscous shear zone is an order of magnitude narrower than the width of the accompanying thermal anomaly. Therefore we need not consider shear heating over a broad zone.

Frictional metamorphism and the Rangitata motwn. During the Rangitata motion, the fault underwest 360 km of slip in some *20* m.y. In the frictional model, if $\tau = \mu\bar{\sigma}_n$, and $\mu = 0.6$ [*Byerlee,* 1978], then if $\bar{\sigma}_n$ is lithostatic, we would expect $\tau \cong 3$ kb at 15 km depth, so that in our model B $\bar{\tau} = 1.5$ kb. If pore pressures are present, $\bar{\tau}$ will be smaller. We accordingly calculated heat flow for models in which $\bar{\tau}$ ranged from 0.5 to 1.5 kb, and v ranged from

2 to 12 cm/yr. For the slower velocities ($v < 8$ cm/yr) the model reaches steady state before the 360 km of motion is complete and an analytical solution was used. At higher velocities the temperatures do not reach steady state and they have been calculated using a finite difference scheme. Both types of calculation are described in detail in the appendix.

Two representative solutions for the temperature distribution at the end of the Rangitata motion are shown in Figure 7. Both began with a background geothermal heat flow of 1 HFU, $\bar{\tau}$ = 1.5 kb and v = 6 cm/yr. Stress model A (Figure ?a) predicts higher temperatures than model B close to the fault at shallow depths. The reverse is true at distances greater than a few kilometers from the fault. Predicted surface heat flow is also shown. The anomaly is concentrated much closer to the fault in model A than in model B. An acceptable model must show the 450° isotherm 4–5 km from the fault and the 300" isotherm 9–12 km from the fault at some depth $11 \leq H \leq 4$ km. Thus, in the models shown in Figure 7, H = 6-8 km. Variations in the assumed value of q_o, the initial geothermal heat flow, will not influence these or subsequent results other than by compressing or expanding the vertical scale in Figure 7, and hence influence values of H. For reasonable values of q_o, say between 0.8 and 1.2 HFU, this will have a negligible effect on our results. The depth H as well as the slip velocity v will therefore be the variable parameters that will affect the value of $\bar{\tau}$ required to produce an acceptable temperature distribution.

In Figure 8 we show $\bar{\tau}$ vs. v plots for both model A and model B, which show the values of $\bar{\tau}$ and v which yield acceptable temperature profiles at the depth H indicated. The greater the value of H, the smaller the value of

$\bar{\tau}$ required to raise the temperatures to appropriate levels. At low velocities, the curves follow lines of $\bar{\tau}v$ = constant, but at higher velocities these curves flatten out and begin to rise at the highest velocities, because at high velocities the temperatures do not have time to reach steady state even though the same amount of heat, $\bar{\tau}u$, is generated by the fault. At velocities higher than about 8 cm/yr, we can find a steady state solution (after fault motion has ceased) that produces an acceptable temperature distribution, but inevitably these solutions predict transient temperatures near the fault at depth E higher than the melting point of these rocks [750°C, according to *Wallace*, 1976]. Since this is not observed, these high velocity models are actually unacceptable. The principal difference between model A and model B is that to match the observations, about 1 km greater uplift is required for model B for the same values of $\bar{\tau}$ and v.

The shear stress minimum for any model is 500 bars for a profile depth of 11 km and is correspondingly higher for shallower depths. Hence we can say that the mean effective shear stress on the fault was at least 500 bars. In fact we favor models with a velocity less than ∿ 8 cm/yr as at higher (non-steady state) velocities the width of the amphibolite zone becomes large with respect to the greenschist zone, and melting is expected along the fault zone at depth E. neither of which is observed. (The rare pegmatite dikes indicate that only a very small amount of the lowest melting fraction of the schists was melted.) Furthermore, the time available for metamorphism becomes very short at the higher velocities. The calculations of the second (Kaikoura) heating episode show that this heating took place in too short a time to produce more than a slight retrograde metamorphism in

the schists. These considerations lead us to conclude that it is very unlikely that $\bar{\tau}$ was less than 750 bars.

Argon depletion and the Kaikoura motion. In discussing the Kaikoura motion we use the same models of stress variation and the same range of values, but the horizontal velocity v is geologically constrained to be within 2.5 to 4 cm/yr. Starting with a background heatflow of 1 HFU we solve the heatflow equation with one side of the fault moving vertically and being planed off by erosion as frictional heating resulting from the horizontal motion takes place on the fault. This finite difference calculation is described in the appendix. The vertical velocity (W) is chosen so that the depth H of the Rangitata metamorphic profile reaches the surface after 5 m.y. or 3 m.y., corresponding to horizontal velocities of 2.5 and 4 cm/yr, respectively. Most of our calculations were done using 2.5 cm/yr as the horizontal velocity. A list of the models tried is given in Table 1.

The temperature history of the profile was followed through the 5 m.y. of motion at various distances from the fault. Some representative temperature histories are shown in Figure 9. In Figure 9a, for example, the results are for a model with stress distribution A, $\bar{\tau}$ = 1.5 kb, moving at 2.5 cm/yr horizontally and 1.67 mm/yr vertically (H = 8.33 km). We plot the temperature history of points at various distances from the fault and an original depth of 8.33 km. The point 1 km from the fault, for example, is heated from 180°C to 275°C after 1 m.y., and subsequently cools. At distances greater than 10 km from the fault, negligible temperature increases occur. In Figure 9b, the results for stress model B are shown with the same values of $\bar{\tau}$ and v. For

model B, temperatures near the fault do not get as high or last as long as in model A, but the opposite is true at greater distances.

We then use these temperature histories and appropriate values for the diffusion coefficient (D_{20}/a^2) and activation energy (E) for argon diffusion from biotite to calculate the fractional loss of argon (F) since the start of motion. (1-F) is directly proportional to K-Ar age for periods as short as 100 m.y. [*Fechtig and Kalbitzer*, 19661. We calculated argon loss for the various models listed in Table 1. For each model we tried a variety of values for D_{20}/a^2 and E *to* determine what values were permissible in order to fit the data. In Figure 10 we show an example. The calculated curves are all for model 1 (Table 1), and we indicate each curve by an upper number, log D_{20}/a^2, and a lower number, E. The family of curves that most closely fits the data (solid circles) is within the cross-hatched region, which encloses possible values for the diffusion parameters for this particular model. It can be seen that a wide range of D_{20}/a^2 and E can be used to fit the rather limited data, though D_{20}/a^2 and E are not independent variables. We could not, however, fit the data with $\bar{\tau}$ = *500* bars using any choice of D_{20}/a^2 or E because for such a low shear stress the temperature history does not vary sufficiently with distance from the fault.

With values of $\bar{\tau}$ = 1 to 1.5 kb. however, the data could easily be fit. In Figure 11 we show the possible values of D_{20}/a^2 and E for models assuming various values of H, $\bar{\tau}$, and W (Table 1). By possible values we mean that they will produce a depletion aureole with almost total argon depletion out to 3-4 km from the fault and almost no depletion at distances greater than 12 km, as the data indicate. Note in Figure 11 that within the range of other parameters, permissible values of D_{20}/a^2 and E show a nearly linear relationship with one another along the lines of B = constant. This simply reflects that

decreasing values of **H** require greater values for argon diffusivity to produce the observed depletion. Direct laboratory measurements of both D_{20}/a^2 and **E** for argon diffusion from biotite are also plotted (x) in Figure 11 [*Frechen and Lippolt*, 1965]. Although in general there are problems with applying experimentally determined argon diffusion parameters to geological situations [*Mussett*, 1969] at least for phlogopite, *Giletti and Tullis* [1977] showed that **E** for argon diffusion is almost independent of pressure and results obtained at high temperatures can be extrapolated to temperatures less than 600°C. If the diffusion parameters of Frechen and Lippolt are the most relevant for *in situ* degassing of argon, they lie near the **H** = 5–6 km curves and hence indicate that the Cenozoic uplift of the Southern Alps was 5–6 km, and that a shear stress $\bar{\tau}$ = 1–1.5 kb produced the heat flow required for the argon depletion. This is consistent with the earlier calculations since if **H** = 5–6 km, 1–1.5 kb of average shear stress are required to produce the metamorphism, even at the highest slip rates (Figure 8). The fact that Rb–Sr ages show a similar depletion aureole near the Alpine fault [*Aronson*, 1965] reflects the fact that the diffusion parameters for Sr diffusion from biotite are similar to those for argon [*Hart*, 1964; *Fechtig and Kalbitzer*, 1966] and is confirmation that thermal degassing is the mechanism responsible for the depletion of ^{40}Ar from these rocks, and thermal diffusion of Sr from the mica phases is the mechanism for the reduction of Rb–Sr ages of mica concentrates from the Haast schists [*Aronson*, 1965]. We note that only a very slight retrograde metamorphism occurred within 1–2 km of the fault during the Kaikoura orogeny, so that

neither bulk recrystallization nor penetrative deformation occurred in the schists during the period of argon depletion [*Grindley*, 1963; *Sheppard et al.*, 1975]. These factors give us confidence in the applicability of our simple, thermally induced, diffusion calculations. We also take confidence in the fact that exactly the same pattern of Rb-Sr and K-Ar depletion are observed in contact metamorphic aureoles [*Hart*, 1964].

We conclude, then, that the argon depletion of the schists could not have been produced with a shear stress as low as 500 bars. At least 750 bars average shear stress is required, and the most likely values, self-consistent with experimentally determined values of the diffusivity of argon and with the metamorphism, are $\bar{\tau}$ = 1-1.5 kb.

DISCUSSION

The K-Ar and Rb-Sr age distribution in the Haast schists could only have been produced by frictional heating on the Alpine fault during the late Cenozoic motion of that fault. An entirely consistent argument shows that the metamorphism of these rocks also resulted from frictional heating during the Mesozoic period of fault motion. Having established that, we can use the argon depletion and metamorphism as independent measures of the frictional heating.

Although it is conceivable that the argon depletion could have been produced by mean shear stresses as low as 750 bars acting on the fault, if we adopt diffusion parameters for argon anywhere near consistent with the experimentally measured values, we must conclude that the shear stresses were at least 1-1.5 kbars, and that the original depth of burial of those rocks was H - 5-6 km.

The metamorphism could have been produced by frictional heating involving shear stresses as low as 500 bars, using the most extreme model permissible. However, if H = 5–6 km, then at least 1–1.5 kb of shear stress are again required, regardless of the velocity of fault motion. There are also several additional arguments that B could not have been as great as 10–11 km. If B were that great, we should expect that 1) melting would be observed close to the fault, which is not observed, 2) the ratio of the width of the amphibolite zone to that of the greenschist zone would be broader than observed, and 3) the volume of sediments derived from the Southern Alps, which presently have an elevation of 3–4 km, would be much greater than observed.

We therefore conclude that it is most unlikely that the mean shear stress on the Alpine fault is less than 1–1.5 kb. Even adopting the most extreme position, our argument is concerned only as to whether it is 750 bars or 1.5 kbars. There is no question that it must be at least one order of magnitude higher than earthquake stress drops. Furthermore, it is important to point out that our estimate is a *minimum* one. That is, we have assumed an efficient system, all other energy losses, through seismic energy release, creation of new surface energy, heat of transformation in metamorphic reactions, and heat loss through convection of ground water, have been neglected, For our particular problem, we do not believe that the latter is significant, since the simple pattern of metamorphic zonation and K–Ar ages with respect to the fault demonstrate that conduction is the principal heat transfer process, at least at the depths of interest here.

Our weakest assumption concerning the history of fault motion is that the entire 120 km offset of the lamprophyre dikes took place after the onset of uplift of the Southern Alps in the Kaikoura orogeny. If the transcurrent

component of fault slip began prior to that, we would have to reduce the mean slip velocity in our calculations, and consequently increase the value of $\bar{\tau}$ required to produce the argon depletion. If we assume it took place in a shorter period of time than 3 m.y. (Model 7, Table 1) we will again find a non-steady state solution which will require a higher value of $\bar{\tau}$. Furthermore, the actual offset of the dike swarm is somewhat uncertain, owing to the difficulty in identifying the boundary of the swarm. Published values range from 100 to 160 km; we used the average and most quoted value of 120 km. This range of uncertainty, however, will not significantly affect our results.

Several other observations also suggest, quite independently, the existence of high shear stresses on the Alpine fault. Pseudotachylites occur commonly within the mylonite zone in lenses as wide as 3 cm [*Wallace*, 1976; R. H. Sibson, personal communication, 19781. The presence of these rocks probably indicates partial fusion during seismic slip. Although if the particle velocities and displacements during a given earthquake are large, shear stresses need not be on the order of kilobars to produce incipient fusion [*McKenzie* and *Brune*, 1972; *Wallace*, 19761, the common occurrence of these rocks is generally indicative of high shear stresses [*Sibson*, 1975]. Furthermore, preliminary transmission electron microscopic studies of the dislocation densities and grain size of the mylonites from the Alpine fault are indicative of shear stresses on the order of a kilobar (S. White, personal communication, 1978).

If our model for and assumptions concerning the frictional metamorphism (Rangitata orogeny) and argon-depletion (Kaikoura orogeny) of the Haast schists is correct, a substantial asymmetric heat flow anomaly should exist over the Alpine fault, the asymmetry being due to the differential uplift of

the Southern Alps. The absence of a heat flow anomaly localized to the San Andreas fault (across a dimension approximately twice the depth of frictional heating) has led *Brune et al.* [1969] and *Lachenbruch and Sass* [1973] to conclude that $\bar{\tau}$ over the upper 15 to 20 km of the San Andreas fault is no more than several hundred bars. This is a substantially smaller frictional stress than our *minimum* estimate for the Alpine fault. On the basis of the very similar frictional strengths of crustal rocks [e.g., *Byerlee*, 1978], it is difficult for us to accept that the frictional strength of crustal fault zones vary by an order of magnitude (or more). except in those cases where (1) nearly lithostatic fluid pressures reduce the effective confining pressure essentially to zero, possibly the case for the *200* km long, aseismically slipping section of the San Andreas fault in central California [*Irwin* and *Barnes*, 1975] or (2) the strength of the fault zone is locally dominated by low strength, high hydration number clay minerals such as vermiculite and illite, perhaps also the case for the creeping section of the San Andreas fault in central California since vermiculite and illite are not observed to result in stick-slip.

There are, however, several additional factors not included in the thermal models of *Brune et al.* [1969] and *Lachenbruch* and *Sass* [1973], which complicate their interpretation. It is now becoming apparent for much of California that the relative motion between the Pacific and Americas plates in post-early Miocene times has not been confined to the present day San Andreas fault but has been distributed over a series of subparallel faults in a zone some *100* km wide. Thus from Point Arguello to Bodega Bay in cen-

tral California, extensive slivering of the Salinian block has occurred [*Johnson and Normark*, 19741, with 115 km of right-lateral motion in post-early Miocene times for the San Gregorio-Hosgri fault [*Graham and Dickinson*, 19781, 50 km of post-Miocene slip on the Rinconada fault [*Graham*, 19781, and suspected slip on the offshore Santa Lucia bank fault [*Silver et al.*, 19781 and Nacimiento fault. Most of the motion on the San Andreas fault did not occur until the last 5-6 m.y. [*Graham and Dickinson*, 1978], a figure close enough to the thermal time constant such that a well developed heat flow anomaly may not yet be recognizable at the surface or may be blurred by thermal anomalies produced by the other active fault strands mentioned. A similar situation exists in southern California where the present active strand of the San Andreas fault has probably only been active since the opening of the Gulf of California [*Atwater*, 19701 and slip is distributed on several strands: the Banning-Mission Creek, San Jacinto, and Elsinore faults.

It is well known that a substantial heat flow anomaly exists in the Coast Ranges of central California [*Lachenbruch and Sass*, 19731 but it is not confined to the immediate region adjacent to the San Andreas fault. The excess heat in this anomaly, which extends 50 km on either side of the San Andreas fault, is enough to account for a kilobar or so of frictional stress at a displacement rate of 5.5 cm/yr. It is certainly possible that the breadth of *this* anomaly is related, at least in the dispersed fault motion described above. Alternatively, as in the case of the unusually low heat flow anomalies with respect to those that "should" exist at mid-ocean rises for reasonable vertical velocities of mass transport from below

[*Hanks*, 1971] and the widely accepted explanation of this discrepancy in terms of hydrothermal circulation [*Anderson* and *Hobart*, 19761, ground water may also interact with the fault zone heat flow anomaly, at least at shallow depth, in such a way as to reduce, broaden, and generally obscure the localized anomaly calculated on the basis of steady-state, thermal conduction models. The coincidence of hot springs with active crustal fault zones [*Barnes et al.*, 1978], while hardly proving this to be the case, certainly does not dissuade us from this possibility, Moreover, the depletion of ^{18}O in metamorphic and plutonic rocks formed within the continental crust [*Taylor*, 19] leave little doubt that they have extensively interacted with ground water. Plainly, however, heat flow measurements in the Southern Alps would be of great value in resolving this dichotomy,

It is obviously of considerable geological importance to ask how common is such frictional metamorphism. There is no question that the Alpine fault is not an isolated case. Elongated linear zones of mylonites, many of which contain cores of magmatic gneiss, which are concentrically surrounded by metamorphic aureoles of just the type studied here have been described in a number of other basement terranes, where they are usually referred to as deep ductile shear zones [*Nicolas* et *al.*, 19771. In fact, the explanation of the origin of such features offered by *Nicolas et al.* [1977] is virtually the same as that employed here, except that they did not have sufficiently well defined boundary conditions to solve the problem quantitatively. In another example, *LeForte* [1975], *Andrieux et at.* [1976] and Ramet *and Allegre* [1976] have argued that frictional heating along the main central thrust of the Himalayas produced the inverted metamorphism of that range and produced

granites by partial melting. *Bird* [1978] calculated the heat generated by frictional heating in that case. He used several indirect arguments[1] to support the assumption that shear stresses along the thrust could not exceed about 200 bars and therefore found that insufficient heat would be generated by this mechanism unless the slip velocity on the thrust exceeds 30 cm/yr, an unlikely high figure. He therefore suggested that some other heat source, such as due to mantle upwelling, must be available. We suggest that if the geologic evidence for shear heating of the Himalayas becomes compelling that the problem may be resolved if the shear stresses on the main central thrust are as high as we find for the Alpine fault. This result has in fact been suggested by *Graham and England* [1976] to account for the inverted metamorphism of the Pelona schists beneath the Vincent thrust in California.

The results we report here are such that it is now important to reexamine the structure and metamorphic history of a variety of shear zones to determine if shear heating does often play an important role in the development of such features and if shear stresses must be generally high along such zones.

[1]The arguments presented by Bird were the paradox first presented by *Hubbert and Rubey* [1959], regarding overthrust faulting, and secondly, the topographical argument discussed by *Jeffreys* [1962]. He differed from Jeffreys on the latter, however, since Jeffreys argued that the topographical expression of the Himalayas requires shear stresses in excess of a kilobar.

ACKNOWLEDGMENTS

Much of this work was done while C. H. Scholz was a visiting scientist at the U. S. Gealogical Survey in Menlo Park, California. This work was supported by the U. S. Geological Survey (P. O. #14629), NASA (NGR 33-008-146), and a Sloan Fellowship. We thank R. H. Sibson and I. W. D. Dalziel for important criticism and suggestions during the course of the work and Prof. Dalziel and R. K. O'Nions for critical reviews.

REFERENCES

Aki, K., Earthquake mechanism, *Tectonophysics, 13,* 423-446, 1972.

Anderson, R. N., and M. Hobart, The relation between heat flow, sediment thickness, and age in the eastern Pacific, *J. Geophys. Res., 81,* 2968-2989, 1976.

Andrieux, J., M. Brunel, and J. Hamet, Metamorphism, granitization, and relations with the Main Central Thrust in Central Nepal, *Proc. Coll. Ecol. Geol. Himalayas,* Paris, 1-6, 1976.

Aronson, J. L., Reconnaissance rubidium-strontium geochronology of New Zealand plutonic and metamorphic rocks, *N. Z. J. Geol. Geophys., 8,* 872-930, 1965.

Atwater, T., Implications of plate tectonics for the Cenozoic tectonic evolution of western North America, *Geol. Soc. Amer. Bull., 81,* 3513-3536, 1970.

Barnes, I., W. P. Irwin, and D. H. White, Global distribution of carbon dioxide discharges and major zones of seismicity, *U. S. Geol. Surv. Water Res. Inv. 78-39,* Open-File Rept., 12 p., 1978.

Bird, P., Initiation of intracontinental subduction in the Himalayas, *J. Geophys. Res., 83,* 4975-4987, 1978.

Brune, J. N., T. L. Henyey, and R. F. Roy, Heat flow, stress, and rate of slip along the San Andreas fault, *J. Geophys. Res., 74,* 3821-3829, 1969.

Byerlee, J., Friction of rocks, *Pure Appl. Geophys., 116,* 615-626, 1978.

Christoffel, D. A., Motion of the New Zealand Alpine fault deduced from the pattern of sea floor spreading, in Recent Crustal Movements, edited by B. W. Collins and R. Raser, Roy. *Soc. R. Z. Bull., 9,* 25-30, 1971

Clark, R. H., and H. W. Wellman, The Alpine fault from Lake McKerrow to Milford Sound, *R. Z. J. Geol. Geophys., 2,* 590-601, 1959.

Davies, G. F., The roles of boundary friction, basal shear stress, and deep mantle convection in plate tectonics, *Geophys. Res. Lett., 5,* 161-164, 1978.

Ernst, W. G., Summary, in *Metamorphism and Plate Tectonics,* edited by W. G. Ernst, Benchmark Papers in Geol., Halsted Press, 372-375, 1975.

Fechtig, H., and S. Kalbitzer, The diffusion of argon in potassium bearing solids, in *Potassium-argon Age Dating,* edited by O. A. Schaeffer and J. Zahringer, Springer-Verlag, Berlin, 68-107, 1966.

Forsyth. D., and S. Uyeda, On the relative importance of the driving force of plate tectonics, *Geophys. J. Roy. Astron. Soc., 43,* 163-200, 1975.

Frechen, J., and U. H. J. Lippolt, Kalium-Argon: Daten zum Alter des Laacher Vulkanismus Rheinterrassen und der Eiszeiten, *Eiszeitalter u. Gegenwart,* 16, 5, 5, 1965.

Giletti, B. J., and J. Tullis, Studies in diffusion, IV, Pressure dependence of Ar diffusion in phlogopite mica, *Earth Planet. Sci. Lett., 35,* 180-183, 1977.

Graham, S. A., Role of Salinian block in evolution of San Andreas fault system, California, *Am. Assoc. Pet. Geol. Bull., 63,* 2214-2231, 1978.

Graham, S. A., and W. R. Dickinson, Evidence for 115 km of right slip on the San Gregorio-Hosgri fault trend, *Science, 199,* 179-181, 1978.

Graham, C. M., and P. C. England, Thermal regimes and regional meta in the vicinity of overthrust faults: An example of shear heatin inverted metamorphic zonation from southern California, *Earth Pla Lett.*, *31*, 142–152, 1976.

Grindley. G. W., Structure of the Alpine schists of South Westland, Southern Alps, New Zealand. *N. Z. J. Geol. Geophys.*, *6*, 872-930, 1963.

Hamet, J., and C.-J. Allegre, Rb-Sr systematics in granite from central Nepal, *Geology*, *4*, 470-472, 1976.

Hanks, T. C., Model relating heat flow values near, and vertical velocities of mass transport near, oceanic ridges, *J. Geophys. Res.*, *76*, 537-544, 1971.

Hanks, T. C., Earthquake stress drops, ambient tectonic stresses and stresses that drive plates, *Pure Appl. Geophys.*, *115*, 441-458, 1977.

Harper, C. T., and C. A. Landis, K-Ar ages from regionally metamorphosed rocks, South Island, New Zealand, *Earth Planet. Sci. Lett.*, *2*, 419-429, 1967.

Hart, S. R, The petrology and isotopic mineral age relations of a contact zone in the Front Range, Colorado, *J. Geol.*, *72*, 493-519, 1964.

Hayes, D. E., and M. Talwani, Geophysical investigations of the Macquarie Ridge complex, in Antarctic Oceanology II, The Australian-New Zealand Sector, Washington, D.C., edited by D. E. Hayes, *Am. Geophys. Union Antarctic Res. Ser. 19*, 211–234, 1972.

Hubbert, M. K, and W. W. Rubey, Role of fluid pressure in mechanics of over-thrust faulting, *Geol. Soc. Amer. Bull.*, *70*, 115-145, 1959.

Hurley, P. M., H. Hughes, W. H. Pinson, snd H. W. Fairbairn, Radiogenic argon and strontium diffusion parameters in biotite at low temperatures observed from Alpine fault uplift in New Zealand, *Geochim. et. Cosmochim. Acta.*, *26*, 67-80. 1962.

Irwin, W. P., and I. Barnes, Effect of geologic structure and metamorphic fluids on seismic behavior of the San Andreas fault system in central and northern California. *Geology, Dec.*, 713-716, 1975.

Jeffreys, H., *The Earth*, 4th Edit., Cambridge, pp. 206-207, 1962.

Johnson, J. D., and W. R. Normark, Neogene tectonic evolution of the Salinian block, west-central California, *Geology*, *2*, 11-14, 1974.

Kanamori, H., and D. L. Anderson, Theoretical basis of some empirical relations in seismology, *Bull. Seismol. Soc. Amer.*, *65*, 1073-1096, 1975.

Lachenbruch. A. H., and J. H. Sass, Thermo-mechanical aspects of the San Andreas fault system, in *Proc. Tect. Prob. San Andreas Fault System*, Stanford Univ. Publ. Geol. Sci. XX, 192-205, 1973.

Landis. C. A., and D. G. Bishop, Plate tectonics and regional stratigraphic-metamorphic relations in the southern part of the New Zealand geosyncline, Geol. *Soc. Amer. Bull.*, *83*, 2267-2284, 1972.

LeForte, P., Himalayas: the collided range, *Amer. J. Sci.*, *275-A*, 1-44, 1975.

Mason, B., Potassium-argon ages of metamorphic rocks and granites from Westland New Zealand. *N. Z. J. Geol.* Geophys., *4*, 352-356, 1961.

Mason, B., Metamorphism in the Southern Alps of New Zealand, *her. Mus. Nat. Hist. Bull.*, *123*, 211-248, 1962.

McKenzie, D. P., and J. N. Bruen, Melting of fault planes during large earthquakes, *Geophys. J. Roy. Astron. Soc.*, *29*, 65-78, 1972.

Mussett, A. E, Diffusion measurements and the Potassium-argon method of dating, *Geophys. J. Roy. Astron. Soc., 18,* 257-303, 1969.

New Zealand Geological Survey, Geological maps of New Zealand, 1:250,000 series, 1965.

Nicolas, A, J. L. Bouchez, J. Blaise, and J. P. Poirier, Geological aspects of deformation in continental shear zones, *Tectonophysics, 42,* 55-73, 1977.

Reed, J. J., Mylonites, cataclastites, and associated rocks along the Alpine fault, South Island, New Zealand, *N. Z. J. Geol. Geophys., 7,* 645-684. 1964.

Scholz, C. A, A discussion of the state of shear stress on faults, in *Proc. Conf. Exp. stud. Friction with Appl. to Earthq. Pred.,* U. S. Geol. Survey, 1977.

Scholz, C. H., J. M. W. Rynn, R. W. Weed, and C. Frohlich, Detailed seismicity of the Alpine fault and Fiordland region, New Zealand, *Geol. Soc. Amer. Butt., 84,* 3297-3316, 1973.

Sheppard, D. S, C. J. Adams, and G. W. Bird, Age of metamorphism and uplift in the Alpine schist belt, New Zealand, *Geol. Soc. Amer. Bull., 86,* 1147-1153, 1975.

Sibson, R. H., Generation of pseudotachylite by ancient seismic faulting, *Geophys. J. Roy. Astron. Soc., 43,* 775-794, 1975.

Silver, E, D. S. McCulloch, and J. R. Curray, Marine geology and tectonic history of the central California continental margin, in press, 1979.

Suggate, R. P.. The Alpine fault, *Roy. Soc. N. Z. Trans., 2,* 105-129, 1963.

Suggate. R. P., The Paringa formation, Westland, New Zealand, *N. Z. J. Geol. Geophys., 11,* 345-355, 1968.

Taylor, H. D., Water/rock interactions and the origin of H_2O in granitic batholiths, *J. Geol. Soc. (Lond.)*, *133*, 509-558, 1977.

Thatcher, W., and T. C. Hanks, Source parameters of southern California earthquakes, *J. Geophys. Res.*, *78*, 8547-8576, 1973.

Wallace, R. C., Partial fusion along the Alpine fault zone, New Zealand, *Geol. Soc. Amer. Bull.*, *87*, 1225-1228, 1976.

Watts, A. B., and M. Talwani, Gravity anomalies seaward of deep-sea trenches and their tectonic implications, *Geophys. J. Roy. Astron. Soc.*, *36*, 57-90, 1974.

Wellman, H. W., New Zealand Quarternary tectonics, *Geol. Runds.*, *43*, 248-257, 1955.

Wellman, P., and A. Cooper, Potassium-argon ages of some New Zealand lamprophyre dikes near the Alpine fault, *N. Z. J. Geol. Geophys.*, *14*, 341-350, 1971.

Yuen, D. A., L. Fleitout, G. Schubert, and C. Froidevoux, Shear deformation zones along major transform faults and subducting slabs, *Geophys. J. Roy. Astron. Soc.*, *54*, 93-119, 1978.

TABLE 1: Models used for argon depletion calculations.

Model No.	Stress distribution	$\bar{\tau}$ (kb)	H (km)	Duration of fault motion (m.y.)
1	A	1.5	6	5
2	B	1.5	8	5
3	A	1.5	8	5
4	B	1.5	5	5
5	A	1.5	5	5
6	B	1.5	6	5
7	B	1.5	5	3
8	B	1.0	6	5

FIGURE CAPTIONS

Fig. 1 Generalized geological map of the South Island of New Zealand. The schists of special interest to this study are separated into the broad NW trending Otago schists and the Haast schist group, outcropping in the Southern Alps adjacent to the Alpine fault. Data from N. Z. Geol. Surv. (1965) and Landis and Bishop (1962).

Fig. 2 Geology of the Haast schist group in the central Southern Alps from Arthur's Pass to Haast Pass.

Fig. 3 All biotite, hornblende, and whole rock K–Ar ages from the South Island which reflect Rangitata orogenic events are shown in relation to their distance from the Alpine fault (after Sheppard et al., 1975).

Fig. 4 Biotite and whole rock K-Ar ages east of the Alpine fault between Arthur's Pass and Haast Pass. Data sources: "x", Sheppard et al., (1975); open circles, Hurley et al., (1962); triangles, Wellman and Cooper, (1972); closed circle, Mason (1962); square, Harper and Landis, (1967). The 4 m.y. age at 12.5 km from the fault is from an isolated gneiss body and its significance is suspect (see Sheppard et al., 1975).

Fig. 5 A sequence of vertical cross sections across the Alpine fault showing schematically the development of the present features. A) The initial configuration; B) The fault moved 360 km right lateral in the Mesozoic and friction caused an elevation of isotherms near the fault. This produced the metamorphic pattern shown in C). In late Cenozoic, D), 120 km of right lateral motion and H km of vertical motion produced argon depletion of the schists and the present metamorphic outcrop pattern.

Fig. 6 The two distributions of shear stress on the fault assumed in the calculations. In model A, a shear stress, $\bar{\tau}$, acts on the fault from 0.5 to 15.5 km depth. In model B, stress increases linearly with depth from 0.5 to 15.5 km.

Fig. 7 Temperature distributions at the end of the Rangitata period of fault motion for stress models A and B. In both cases $\bar{\tau}$ = 1.5 kbar and v = 6 cm/yr. The surface heat flow predicted by the models is also shown.

Fig. 8 Values of $\bar{\tau}$ vs. v at various assumed depths of burial H, required to produce the observed pattern of metamorphism: a) results for stress model A, b) stress model B. The numbered dots indicate depth, H, for various models which were determined by matching the 300°C and 450°C isotherms with the present surface metamorphic zone boundaries. The determinations of H are subject to uncertainties of about 20%. The crosshatched bands give the values of H for which the values of $\bar{\tau}$ and v are appropriate.

Fig. 9 The temperature history of points at four distances from the fault at an original depth of 8.33. km. In these models $\bar{\tau}$ = 1.5 kb, v = 2.5 cm/yr and w = 1.67 mm/yr. a) Stress model A, b) stress model B.

Fig. 10 Fractional argon loss as a function of distance from the fault for model 1 (Table 1) and various values of log D_{20}/a^2 (upper number) and E (lower number) for diffusion of argon. Dots are observed values, and the family of curves within the crosshatched region are those consistent with the data.

Fig. 11 Permissible values of the diffusion parameters D_{20}/a^2 and E for argon diffusion from biotite that fit the observations for the various models listed in Table 1. Values of D_{20}/a^2 and E fall along curves of constant original depth of burial, H. Direct laboratory values for these constants are shown as X (Frechen and Lippolt, 1965).

Fig. A1 The geometry of the fault zone used for the heat flow calculations.

APPENDIX

A1. *Finite difference scheme*

We solve the heat flow equation in a rectangular region whose RHS is moving in the z direction with velocity W (W is negative if the RHS is uplifted relative to the LHS). Heat is generated along the boundary $x = 0$, $0 < z < D$ (Fig. A1). The equations to be solved are:

LHS :
$$\frac{\partial T}{\partial t} = \frac{\kappa}{\rho c}\nabla^2 T$$

RHS :
$$\frac{\partial T}{\partial t} + W\frac{\partial T}{\partial z} = \frac{\kappa}{\rho c}\nabla^2 T$$

where T is temperature, κ is thermalconductivity, ρ is density and c is specific heat.

We use a simple central-difference finite difference scheme with the following boundary conditions:

$z = 0$	constant temperature (20°C)
$z = A$	constant temperature (to give required geothermal gradient far from fault)
$x = 0$	prescribed heat generation $q(z) = \tau(z) \times v$
$x = \pm L$	zero horizontal heat flux

Typical values for the parameters are:

$L = 40$ km $\qquad A = 30$ km $\qquad$ grid size = 1 km

$\kappa = 0.005$ cal cm^{-1} s^{-1} $\qquad c = 0.2$ cal gm^{-1}

$\rho = 3$ gm cm^{-3}

1 mm $yr^{-1} \leq W \leq 3$ mm yr^{-1}

2.5 cm $yr^{-1} \leq v \leq 4$ cm yr^{-1}

The finite difference scheme has been checked by setting the vertical velocity, W, to zero and running the scheme to a steady state solution (≤ 10 MY). The solution is in satisfactory agreement with the analytic steady state solution (Appendix A2), the maximum differences being about 5%.

A2. *Analytic steady state solutions*

The heat flow equation in the area to one side of the fault with no vertical velocity is:

$$\frac{\partial^2 T}{\partial x^2} + \frac{\partial^2 T}{\partial z^2} = 0 \qquad 0 \leq z \leq A,\ x > 0$$

with boundary conditions

$$T = 0 \qquad z = 0,\ A$$

$$\frac{\partial T}{\partial x} = \frac{-q(z)}{2\kappa} \qquad x = 0,\ h/2 < z < D + h/2$$

$$= 0 \qquad x = 0, \qquad 0 \leq z \leq h/2,\ D + h/2 \leq z \leq A$$

Here $q(z)$ $(= \tau(z) \times v)$ is the heat generated by the fault, so $q/2$ is the heat which flows to each side of the fault. h is the grid spacing used in the finite difference scheme and is introduced here so that the analytic solution corresponds as closely as possible to the numerical one with $W = 0$. The geothermal gradient can be ignored in this calculation as it can simply be added to the analytic steady state solution.

We now look for a solution in the form

$$T = \sum_{1}^{\infty} a_n e^{-n\pi x/A} \sin \frac{n\pi z}{A} .$$

For heat flow model A, $\tau(z) = \bar{\tau}$, and we find

$$a_n = \frac{\bar{\tau} v A}{n^2 \pi^2 \kappa} \cdot \cos \frac{n\pi(h/2)}{A} \cdot (1-(-1)^n).$$

For heat flow model B, $\tau(z) = 2\bar{\tau} \frac{z}{D}$ $\qquad \frac{h}{2} < z < D + \frac{h}{2}$

$= 0$ $\qquad$ otherwise

and we obtain

$$a_n = \frac{2\bar{\tau}vA^2}{n^2\pi^3\kappa D}\left(\sin\frac{n\pi(D+h/2)}{A} - \sin\frac{n\pi h/2}{A}\right)$$

$$- \frac{2\bar{\tau}vA}{n\pi^2\kappa D}\left((D+h/2)\cos\frac{n\pi(D+h/2)}{A} - h/2\cos\frac{n\pi h/2}{A}\right)$$

A3. *Modelling of argon diffusion*

A particular steady state solution (Appendix A2) for the end of the Rangitata orogeny is taken. Then it is run through the finite difference scheme (Appendix A1) for 5 MY with a horizontal velocity of 2.5 cm/yr (or for 3 MY at 4 cm/yr) with a vertical velocity chosen to bring the required metamorphic cross-section to the surface at the end of the motion. These velocities are typically 1 to 2 mm/yr. The temperature history of this surface is followed, then the temperature history curves are interpolated by cubic splines in order to give a sufficiently detailed representation of the temperature for the numerical integration below to converge. About 40 points were required for each curve. The fractional argon loss, F, is calculated as

$$F = \Sigma\Delta F = \sum_{t_i=0}^{N\Delta t} \cdot \left\{\frac{3}{\pi^{3/2}}\sqrt{B}\cdot\frac{1}{\sqrt{t_i}} - \frac{3}{\pi^2}B\right\}\Delta t$$

where Δt is the time step, N is the number of steps, and

$$B = \frac{\pi^2}{a^2}D$$

$$D = D_{20}\, e^{-\left(\frac{E}{R} \cdot \frac{293-T}{293T}\right)}$$

E = activation energy

R = gas constant

$\frac{D_{20}}{a^2}$ is diffusion parameter at 20°C

a is an effective grain size.

This approximate formula is derived from one given by *Fechtig and Kalbitzer* [1966, p. 70] for diffusion from a spherical grain when the initial argon concentration is constant throughout the grain. Their formula gave the fractional loss after time t at constant temperature T as

$$F = \frac{6}{\pi^{3/2}} \sqrt{Bt} - \frac{3}{\pi^2} Bt \;, \quad F < 0.9.$$

To obtain our formula we have differentiated with respect to time to give the fractional argon loss ΔF per time Δt at constant temperature. Then we integrate numerically with variable temperature. This should be sufficiently accurate provided that the argon loss, ΔF, within any timestep is $<< 0.9$.

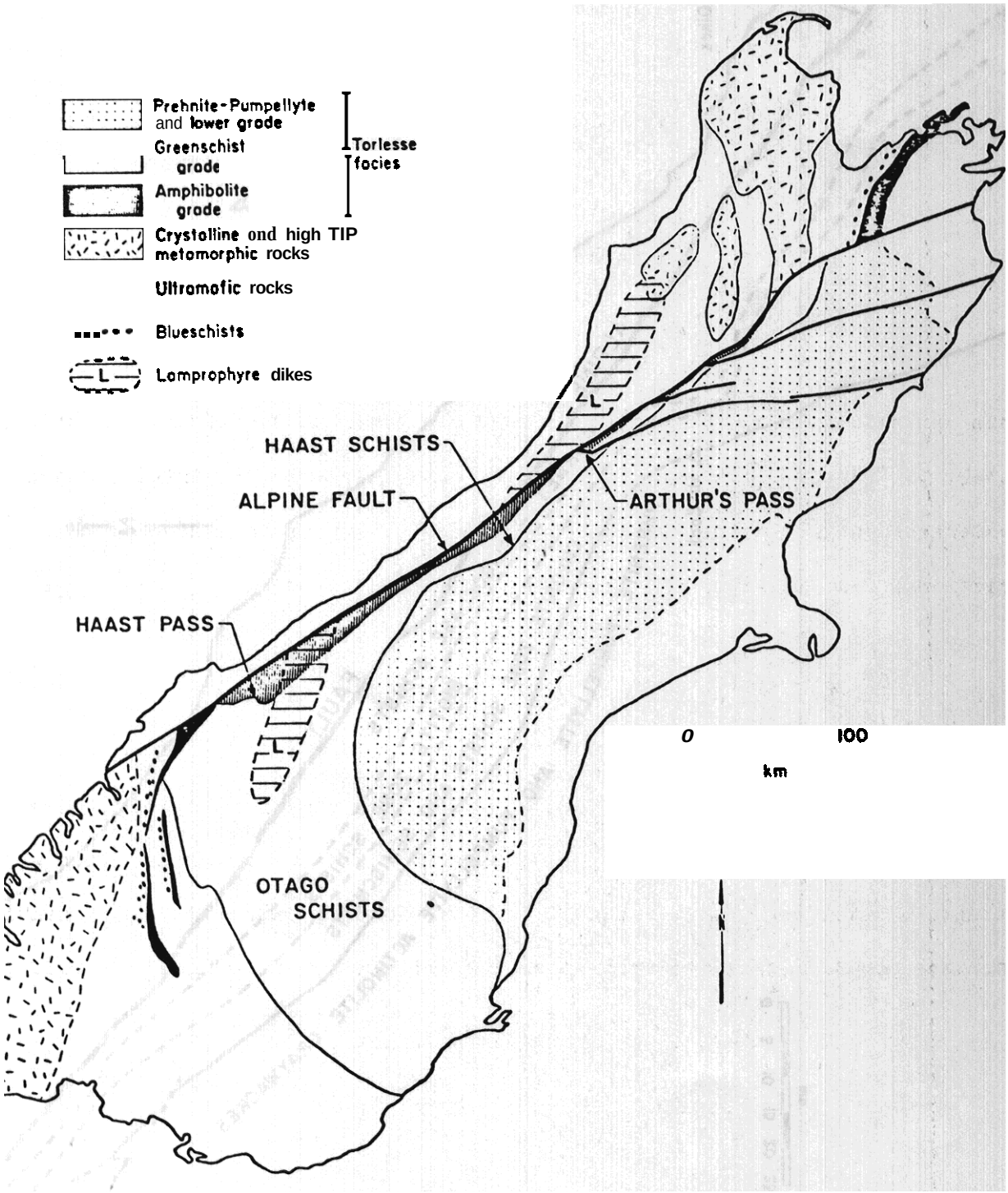
Prehnite-Pumpellyte and lower grade
Greenschist grade
Amphibolite grade
Torlesse facies
Crystalline and high TIP metamorphic rocks
Ultramafic rocks
Blueschists
Lamprophyre dikes
HAAST SCHISTS
ALPINE FAULT
ARTHUR'S PASS
HAAST PASS
OTAGO SCHISTS
0
100
km

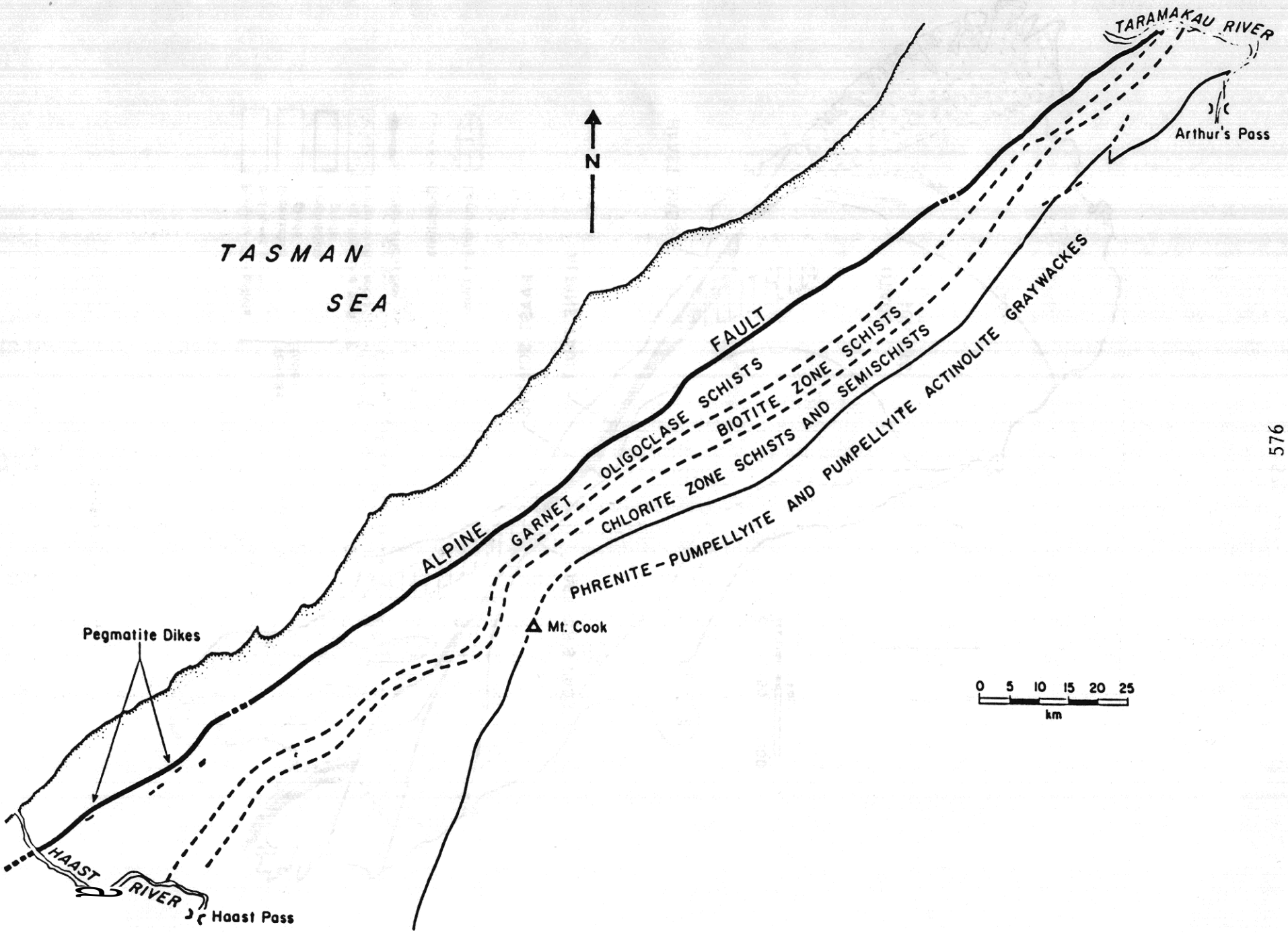
TARAMAKAU RIVER
Arthur's Pass
N
TASMAN
SEA
FAULT
ALPINE
GARNET - OLIGOCLASE SCHISTS
BIOTITE ZONE SCHISTS
CHLORITE ZONE SCHISTS AND SEMISCHISTS
PHRENITE - PUMPELLYITE AND PUMPELLYITE ACTINOLITE GRAYWACKES
Mt. Cook
Pegmatite Dikes
HAAST RIVER
Haast Pass
0 5 10 15 20 25
km

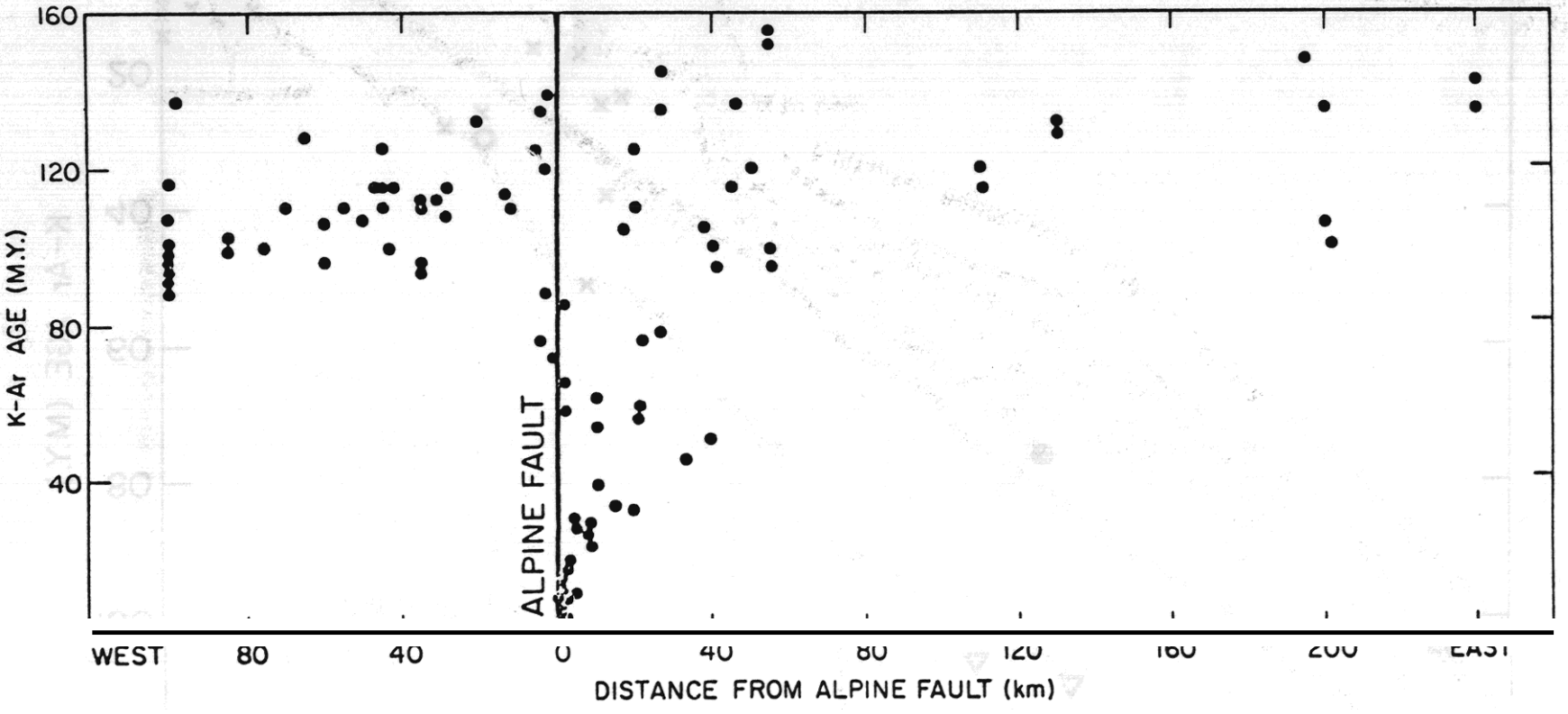
160
120
80
40
K-Ar AGE (M.Y.)
ALPINE FAULT
WEST
80
40
0
40
80
120
160
200
EAST
DISTANCE FROM ALPINE FAULT (km)

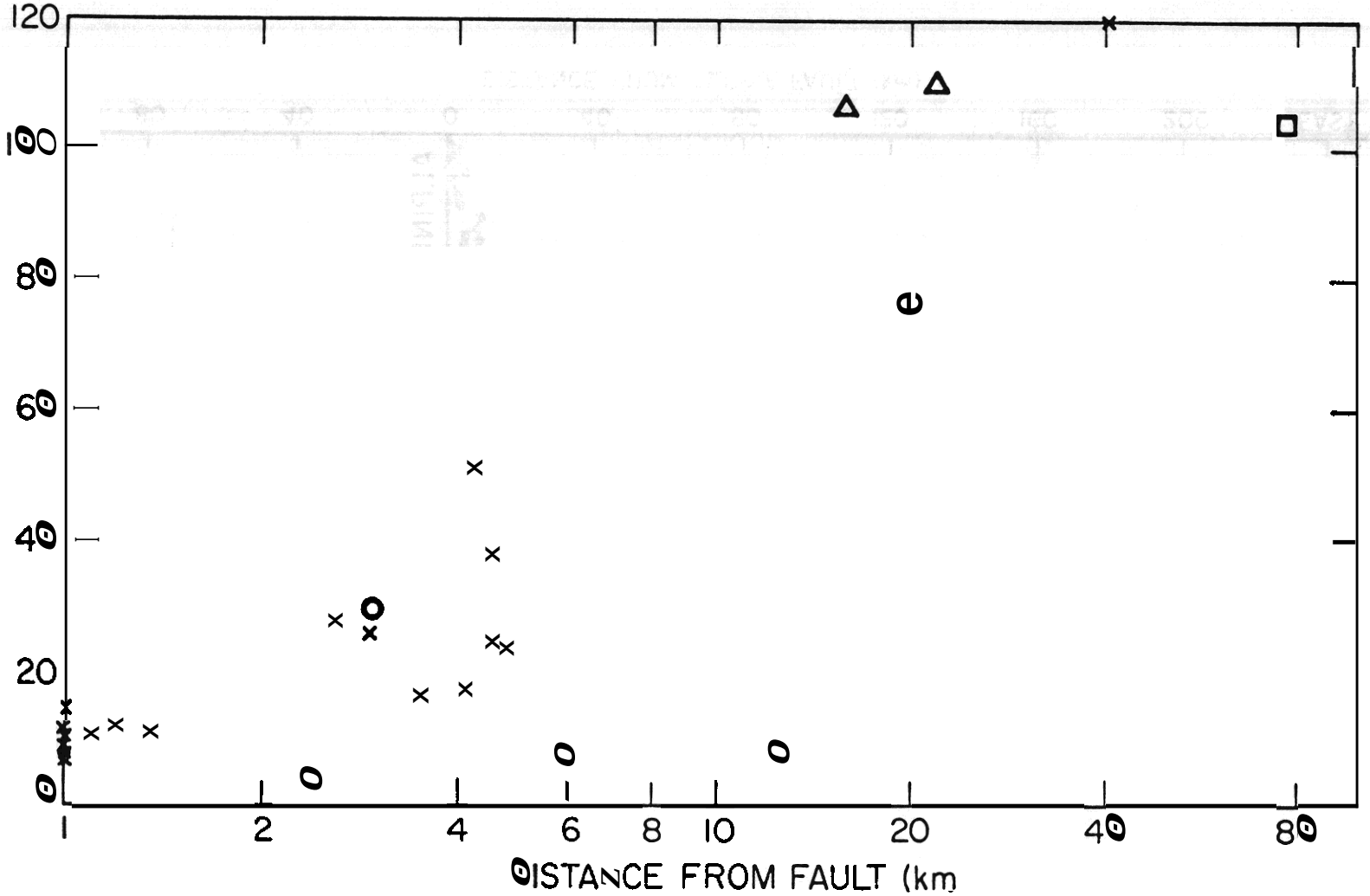
120
100
80
60
40
20
0
1
2
4
6
8
10
20
40
80
DISTANCE FROM FAULT (km

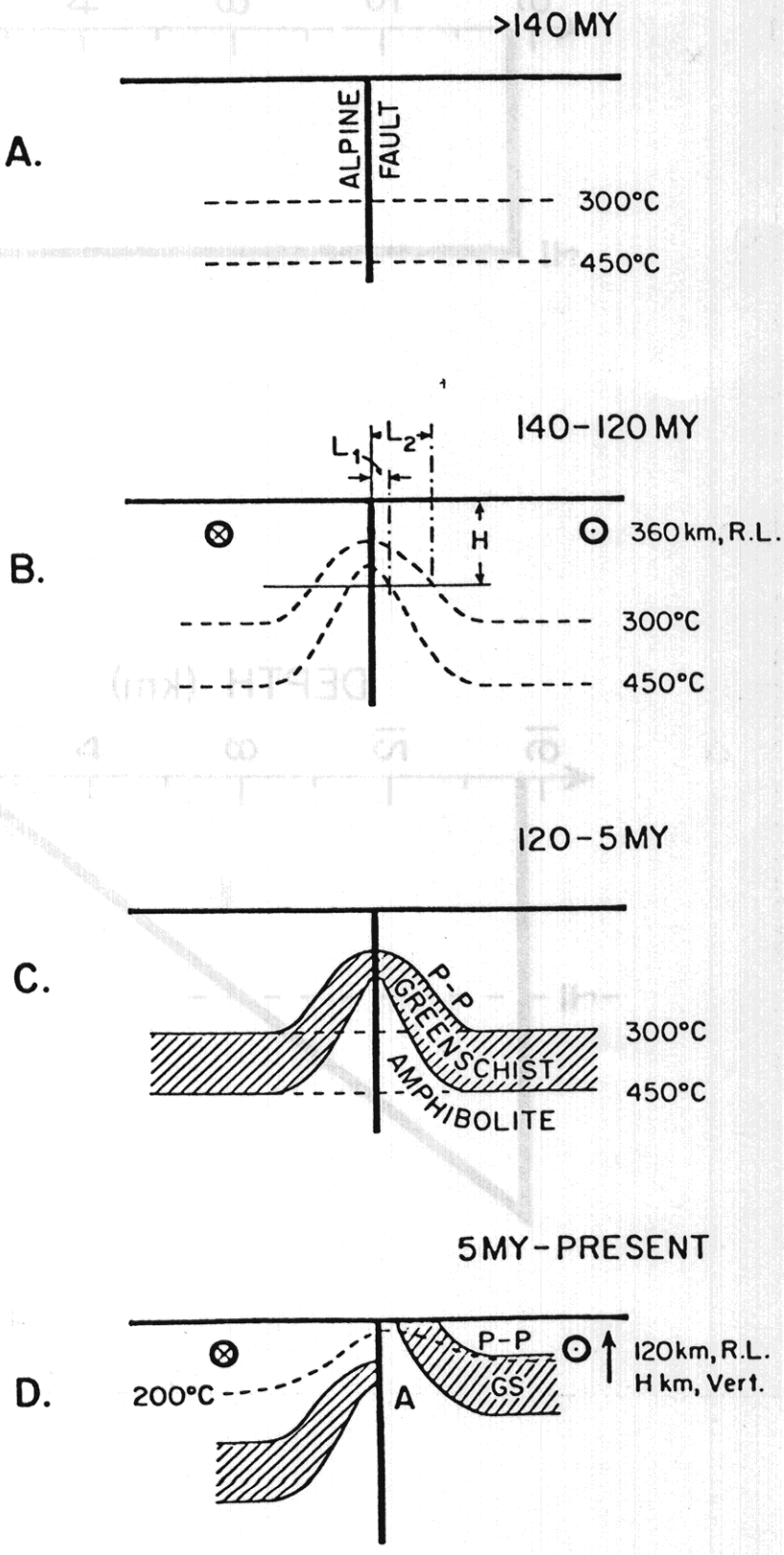
>140 MY
A.
ALPINE
FAULT
300°C
450°C
140-120 MY
B.
L_1
L_2
H
360 km, R.L.
300°C
450°C
120-5 MY
C.
P-P
GREENSCHIST
AMPHIBOLITE
300°C
450°C
5MY-PRESENT
D.
200°C
A
P-P
GS
120km, R.L.
H km, Vert.

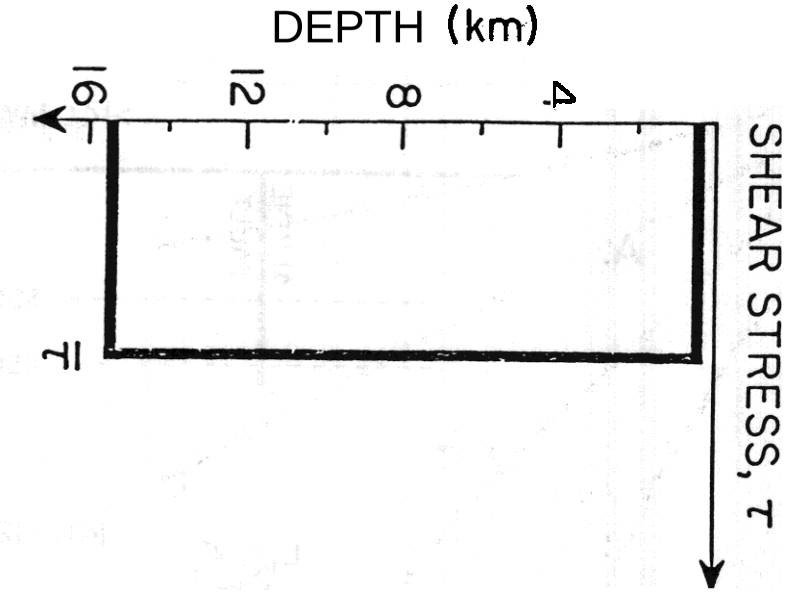
DEPTH (km)
16
12
8
4
τ
SHEAR STRESS, τ

D

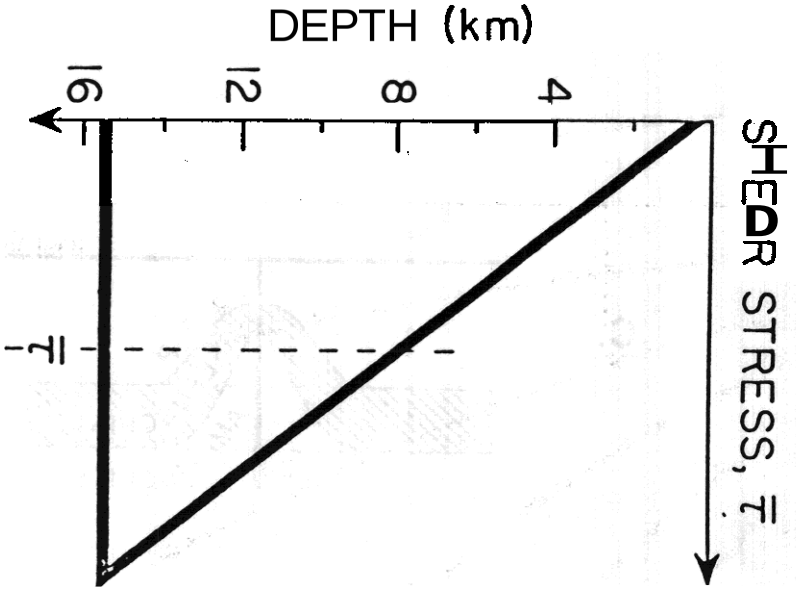
DEPTH (km)
16
12
8
4
τ
SHEAR STRESS, τ

B

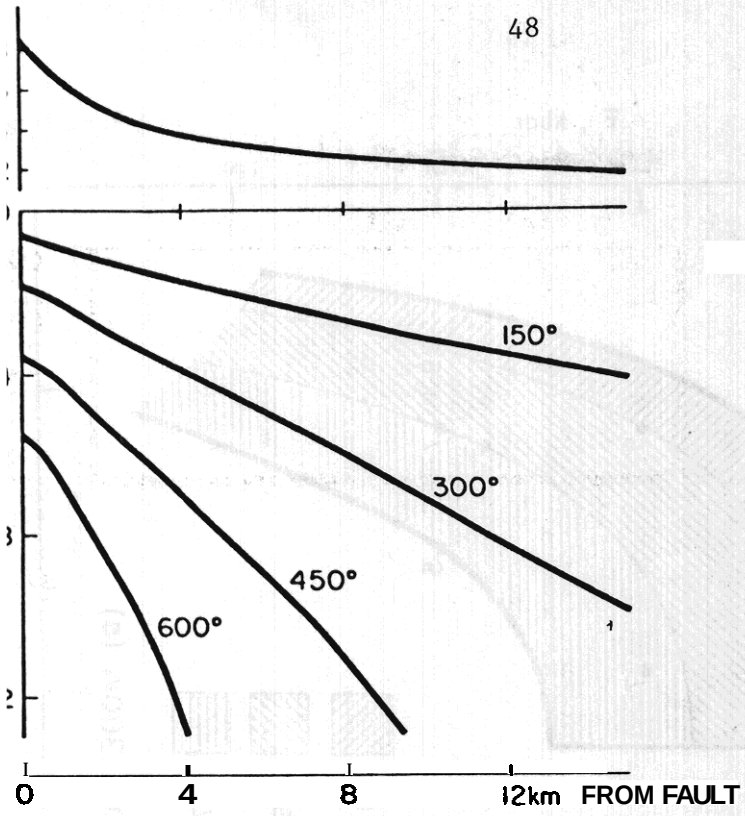
150°
300°
450°
600°
0
4
8
12km FROM FAULT

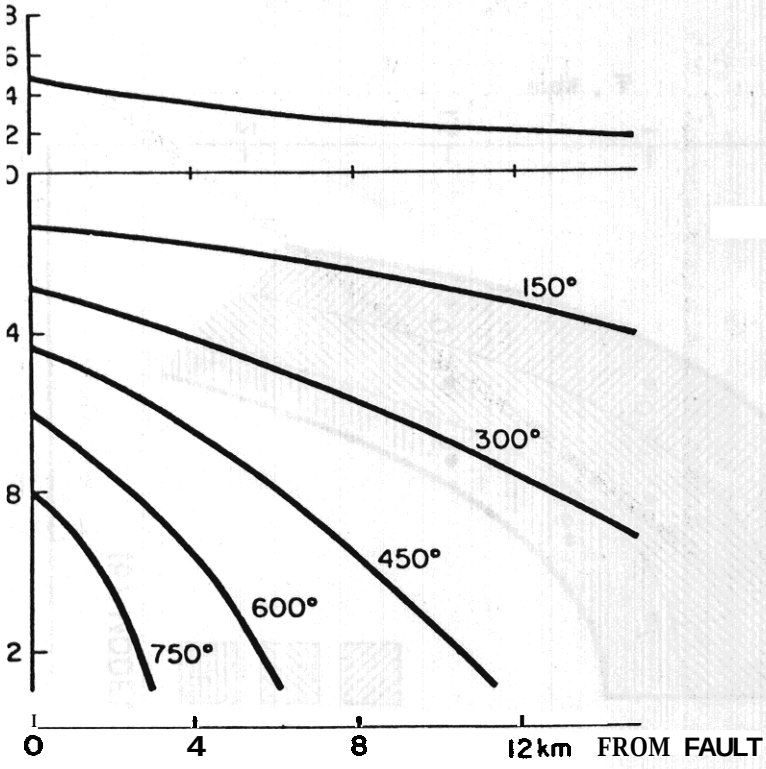
150°
300°
450°
600°
750°
0
4
8
12km FROM FAULT

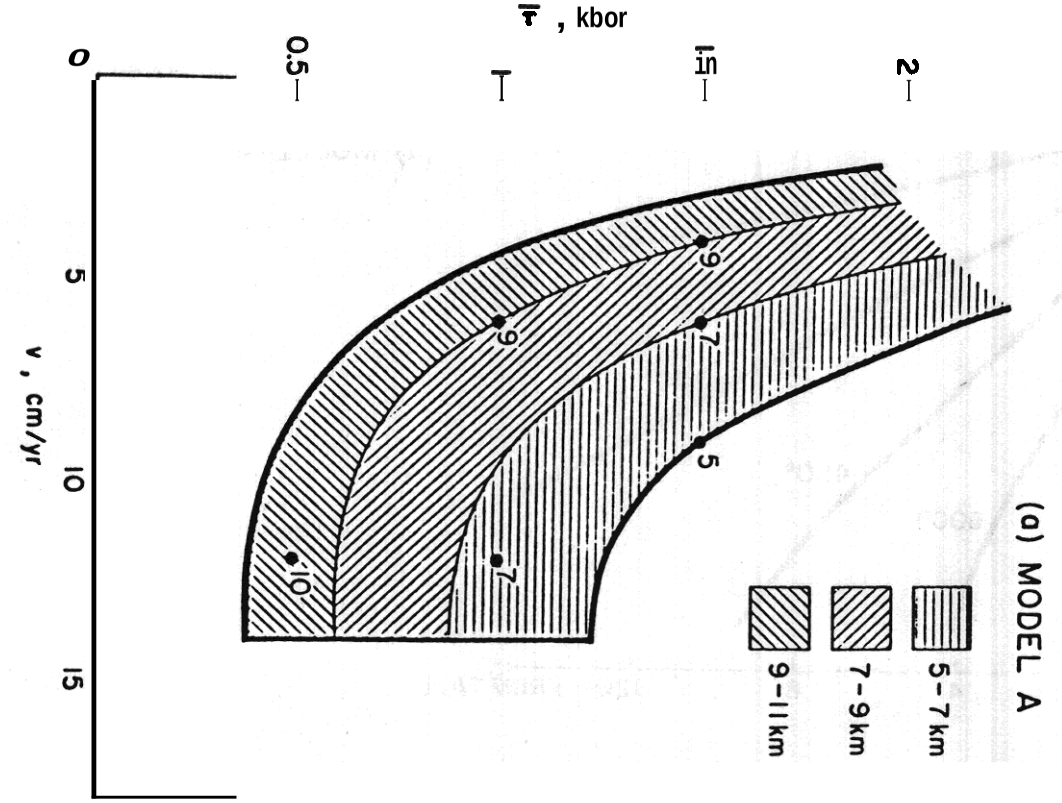
τ̄ , kbor
0
0.5
1
1.5
2
v , cm/yr
0
5
10
15
(a) MODEL A
5-7 km
7-9 km
9-11 km
9
9
7
5
10
7

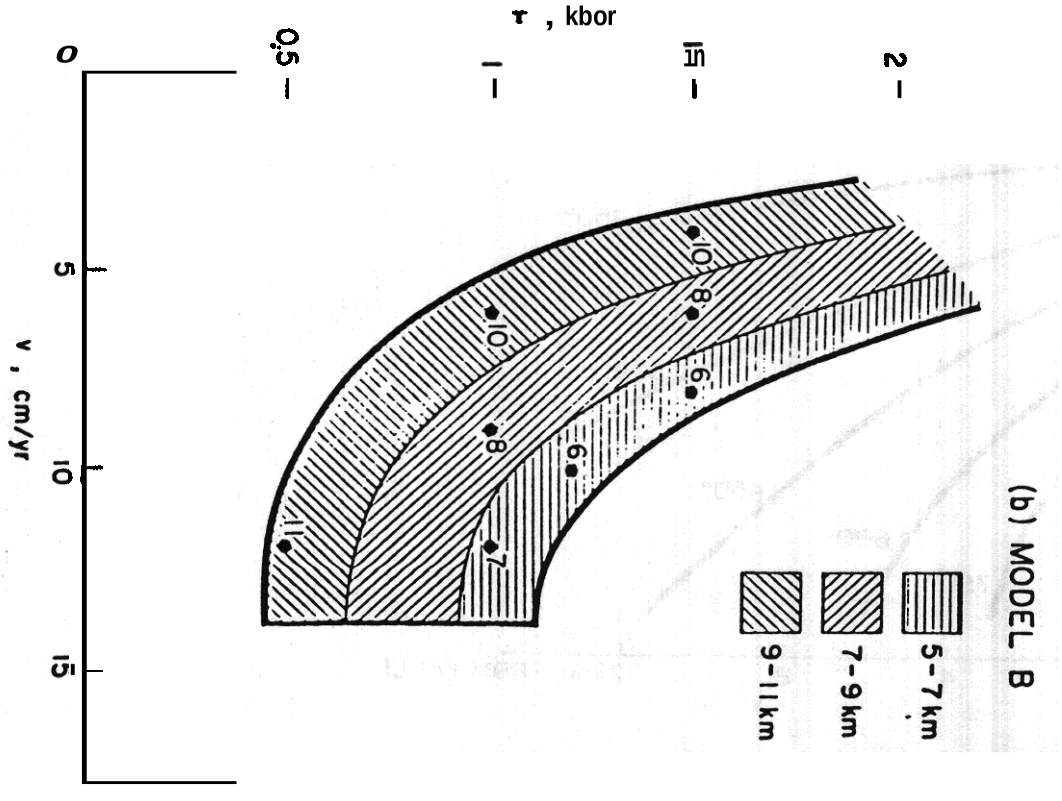
τ̄ , kbor
0
0.5
1
1.5
2
v , cm/yr
0
5
10
15
(b) MODEL B
5-7 km
7-9 km
9-11 km
10
8
10
9
8
6
11
7

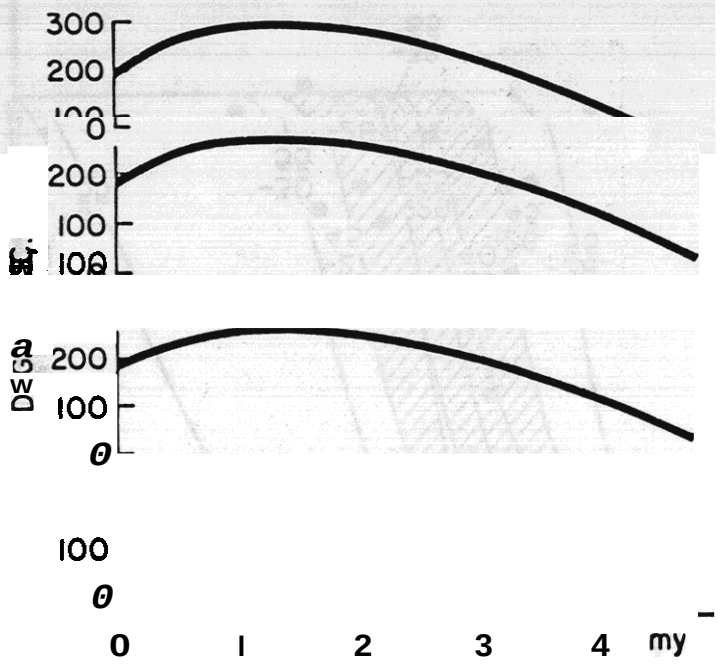

(a) MODEL A

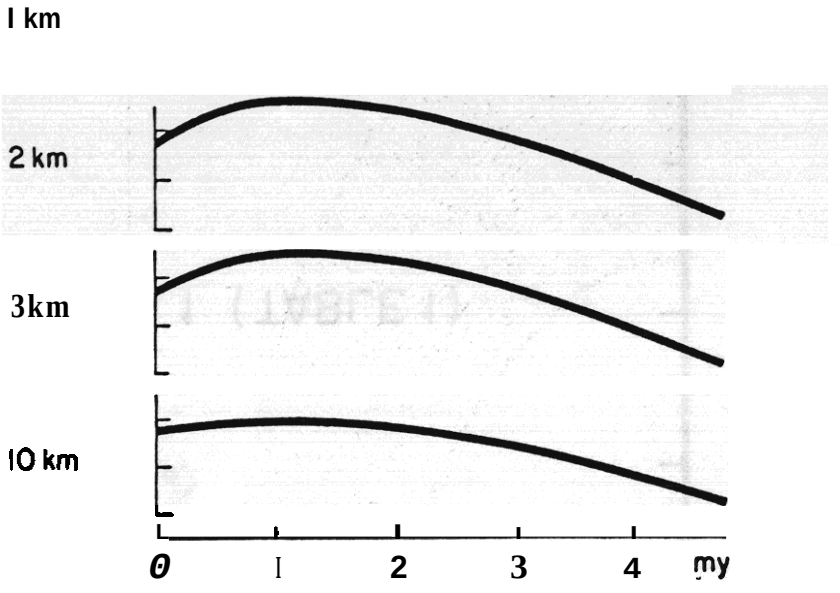

(b) MODEL B

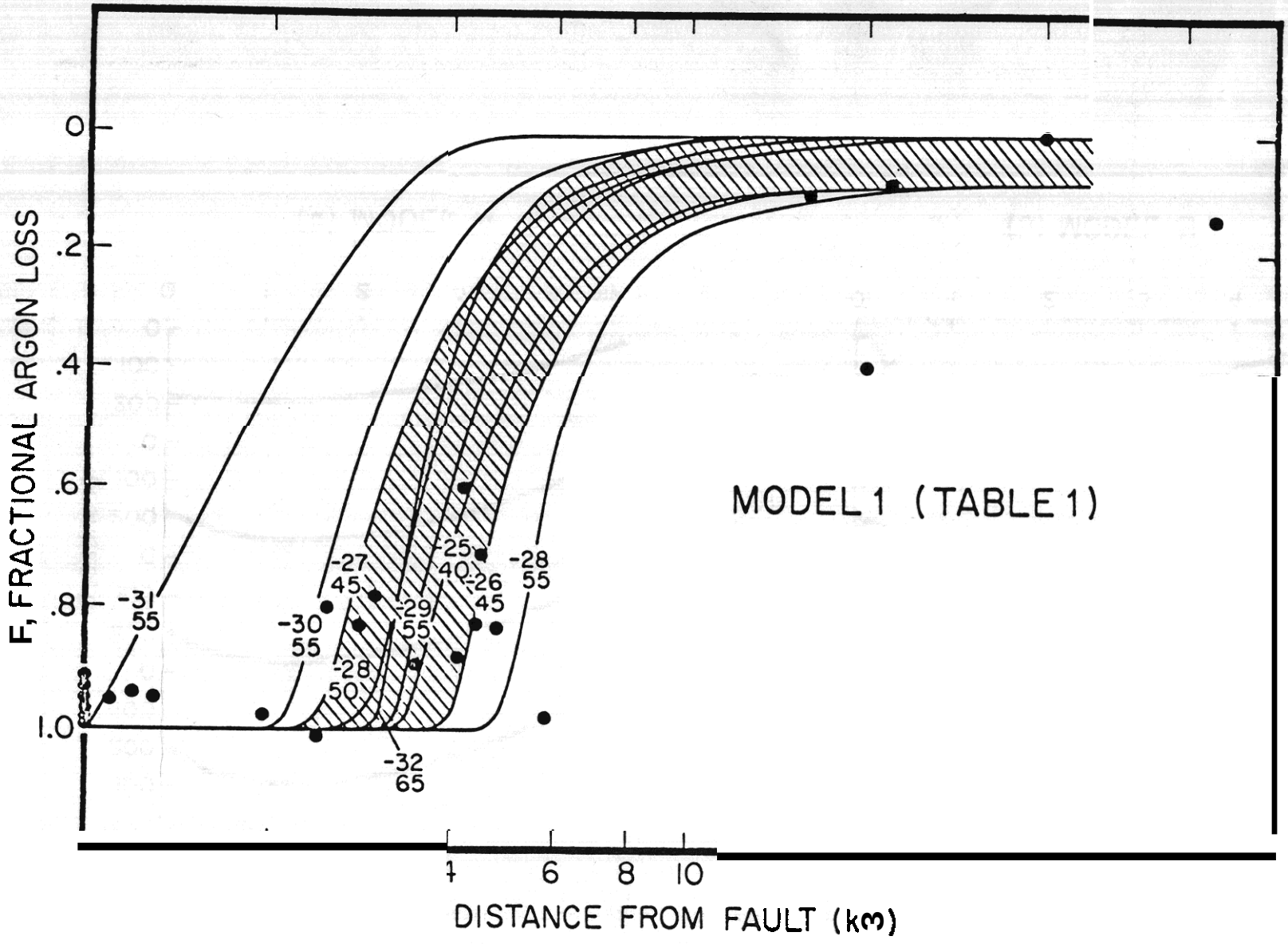
F, FRACTIONAL ARGON LOSS
0
.2
.4
.6
.8
1.0
MODEL 1 (TABLE 1)
-31
55
-30
55
-27
45
-28
50
-29
55
-25
40
-26
45
-28
55
-32
65
1
6
8
10
DISTANCE FROM FAULT (km)

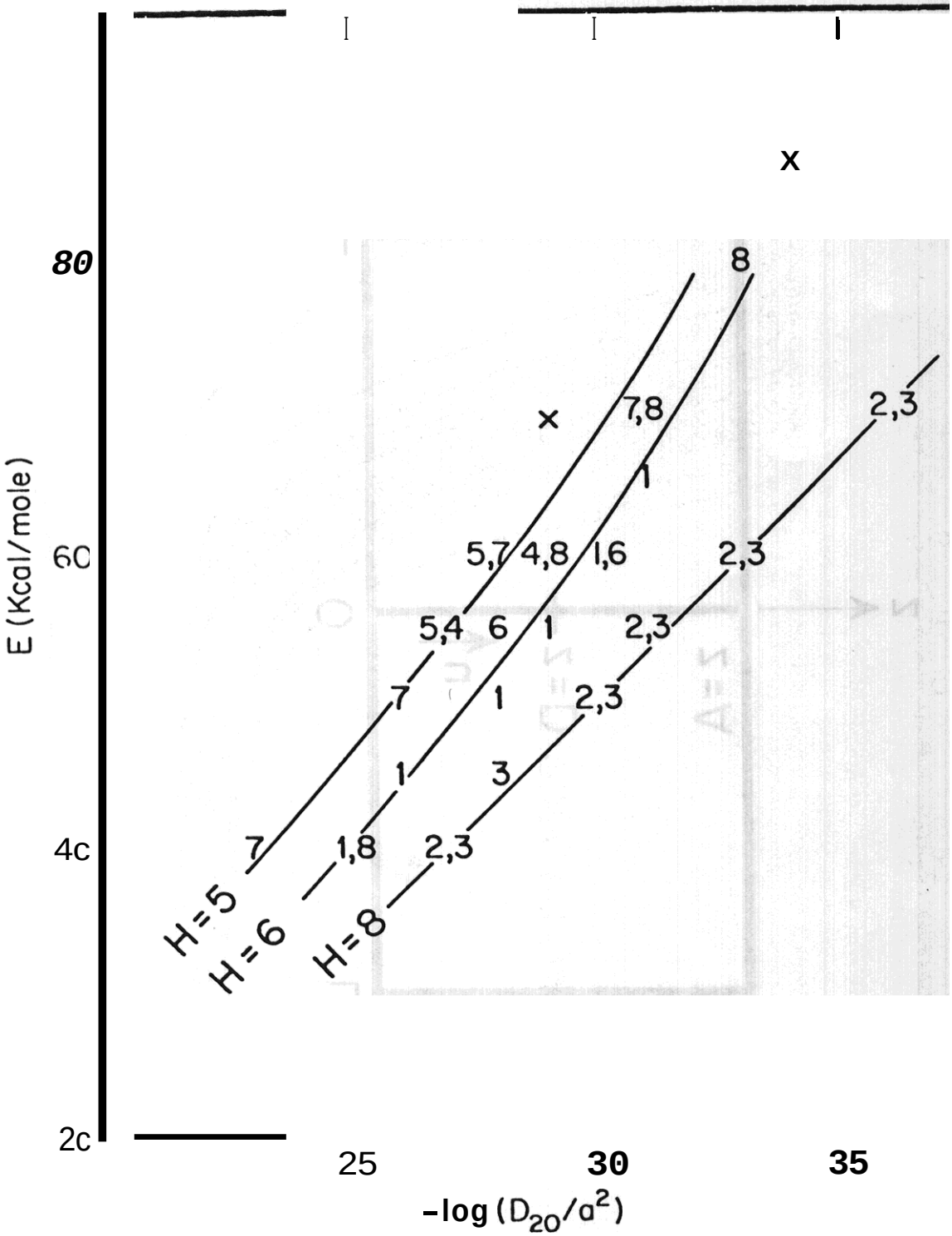
80
60
40
20
E (Kcal/mole)
25
30
35
-log (D20/a2)
H=5
H=6
H=8
8
7,8
5,7
4,8
1,6
5,4
6
2,3
1,8
3

r
0
l
x
u
z=D
v=v
z